

## Particle focusing in a microchannel with acoustic metafluid

Xiaobing Cai, Qiuquan Guo, Gengkai Hu, and Jun Yang

Citation: *Appl. Phys. Lett.* **103**, 031901 (2013); doi: 10.1063/1.4813745

View online: <http://dx.doi.org/10.1063/1.4813745>

View Table of Contents: <http://apl.aip.org/resource/1/APPLAB/v103/i3>

Published by the [AIP Publishing LLC](#).

---

### Additional information on *Appl. Phys. Lett.*

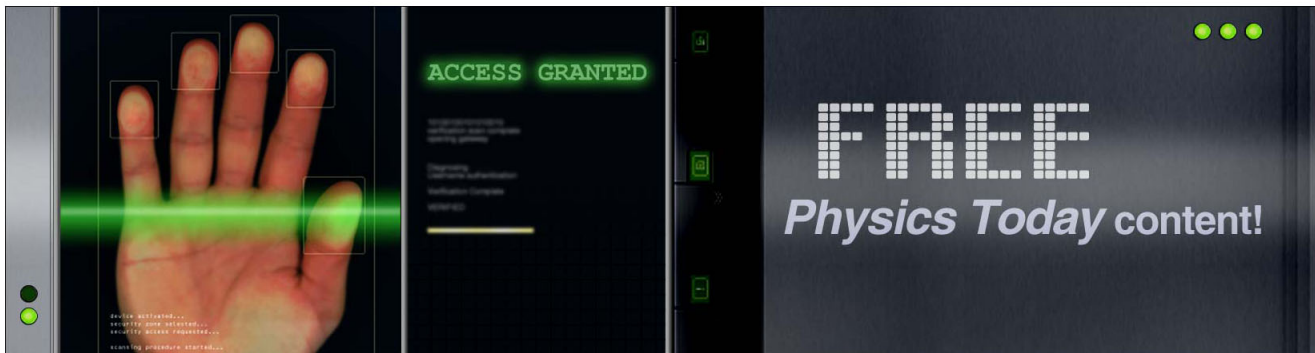
Journal Homepage: <http://apl.aip.org/>

Journal Information: [http://apl.aip.org/about/about\\_the\\_journal](http://apl.aip.org/about/about_the_journal)

Top downloads: [http://apl.aip.org/features/most\\_downloaded](http://apl.aip.org/features/most_downloaded)

Information for Authors: <http://apl.aip.org/authors>

## ADVERTISEMENT



## Particle focusing in a microchannel with acoustic metafluid

Xiaobing Cai,<sup>1,2</sup> Qiuquan Guo,<sup>1</sup> Gengkai Hu,<sup>2</sup> and Jun Yang<sup>1,a)</sup>

<sup>1</sup>*Department of Mechanical and Materials Engineering, The University of Western Ontario, London, Ontario N6A 5B9, Canada*

<sup>2</sup>*School of Aerospace Engineering, Beijing Institute of Technology, Beijing 100081, People's Republic of China*

(Received 29 March 2013; accepted 24 June 2013; published online 15 July 2013)

This work proposed a method of particle focusing by acoustic waves in a microfluidic channel with meta-structures. The channel was first filled by homogeneous metafluid possessing negative bulk modulus or density, mechanism and efficacy of particle focusing in such channel have been studied. Then as a realization, a structural microchannel composed of acoustic resonant elements has been proposed, which generated similar acoustic field gradient as that in homogeneous metafluid. Accordingly, particle movements in the structural microchannel were investigated and particle focusing was also achieved. The proposed particle focusing method is independent on the type of incident wave and microchannel's size. © 2013 AIP Publishing LLC.

[<http://dx.doi.org/10.1063/1.4813745>]

Manipulation of particles into a confined region has significant applications for lab-on-a-chip devices, therefore, a variety of particle focusing methods have been proposed, based on mechanisms ranging from hydrodynamic<sup>1-3</sup> to electro-osmosis,<sup>4-7</sup> dielectrophoresis,<sup>8-10</sup> magnetophoresis,<sup>11</sup> and acoustophoresis.<sup>12-14</sup> These technology achievements are effective in various circumstances and has brought many interesting applications, and yet still require necessary improvement in some cases. For example, electro-osmosis, dielectrophoresis, and magnetophoresis methods could cause potential damage to target particles like soft cells, making them not preferable in doing sensitive experiments, such as reproductive cell operations.<sup>15</sup> A probably less damaging approach is particle focusing by acoustophoresis. However, it usually takes into effect only when ultrasound standing waves build up in a microchannel, and thus, requires the wavelength of the ultrasound to have a strict relation to the size of the microchannel, which may become a problem when the channel is much wider than the wavelength. One case is in cell sonoporation, ultrasound is adopted for both cell manipulating and cell membrane rupturing, while the latter needs a wavelength much smaller than the former.<sup>16</sup>

In order to overcome this restriction, in this paper, we propose a modified avenue to achieve particle focusing by taking advantage of unique properties of metamaterials. In recent decade, a category of metamaterials emerge, which reveal abnormal properties, and thus, attract great attentions of scientists from various fields.<sup>17-19</sup> Their acoustic counterparts have been proposed and realized<sup>20-25</sup> recently, and also exhibit unconventional behavior, such as transforming propagating waves into evanescent ones.<sup>22</sup> The evanescent wave exponentially decreases after penetrating into a single negative metamaterial, and thus, can be readily used to create a nodal position or stable region right at the center of a channel to confine particles. Due to its character of exponential

decaying, the gradient of evanescent field could be much higher than that of a standing wave field that simply varies sinusoidally. With a higher field gradient, particles in evanescent field are accordingly experiencing greater acoustic radiation forces,<sup>26-29</sup> and are driven to move more swiftly.

In this work, a model demonstrates particle focusing movement prompted by acoustophoresis force in a channel filled by density-negative or bulk modulus-negative metafluid has been studied. In a homogeneous metafluid analysis, all particles achieved to be confined in a region less than one tenth of the wavelength after 20 s. Then particle movement in a microchannel with resonant structures below, which make it equivalent to a homogeneous metafluid with negative bulk modulus, have also been studied.

Figure 1 shows the sketch of microfluidic channel used for particle focusing. A microfluidic channel inside Polydimethylsiloxane (PDMS) is demonstrated with one inlet and one outlet, realized by needles sticking into the PDMS and pushed by syringe pumps to ensure the fluid flows. In middle part of the channel, piezoelectric plates are placed onto the two side walls to excite acoustic waves into the fluid. Resonant structures are designed beneath the middle part, which are fluid tanks connect to the channel via small necks. A sectional view of the middle part is shown in Fig. 2. By resonating with the incident ultrasound wave, these structures will push fluid back to the channel even under acoustic pressure, thus, makes the fluid in the channel responding to the acoustic fluctuation in a negative way. Particles are released into the channel from the inlet with a dispersive pattern, and expected to be confined in the center region during traveling through the middle part of the channel.

To enable a clear illustration of the microfluidic channel, let us assume there are no resonant structures under the middle part of the channel, in stand, a negative density is assigned to the fluid within this part. In this way, the distribution of the pressure fluctuation due to ultrasound wave perturbation can be calculated. Assuming the ultrasound waves excited by the actuators are plane waves, then the pressure field can be expressed by<sup>30</sup>

<sup>a)</sup>Author to whom correspondence should be addressed. Electronic mail: [jyang@eng.uwo.ca](mailto:jyang@eng.uwo.ca). Telephone: 1-519-661-2111 ext. 80158. Fax: 1-519-661-3020.

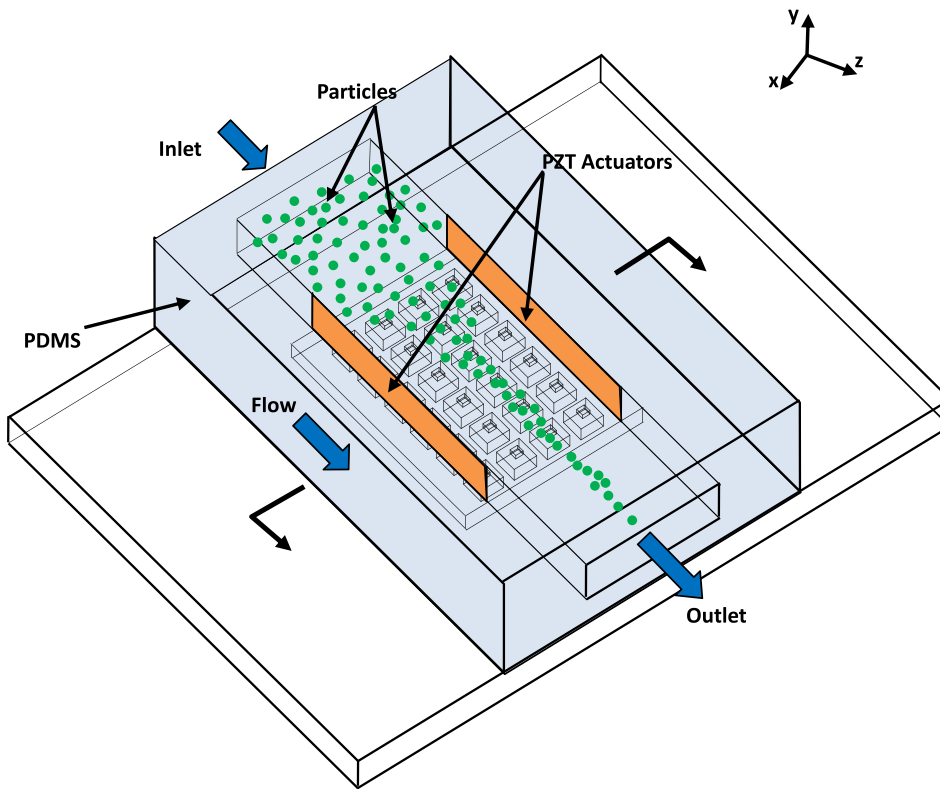


FIG. 1. The sketch of particle focusing in a microchannel with acoustic resonant elements.

$$P = p_0[\exp(-ik(x - L/2)) + \exp(ik(x + L/2))], \quad (1)$$

where  $p_0$  is the pressure amplitude generated by the actuators,  $k = \omega\sqrt{\rho/K}$  is the wave vector, and  $\omega$ ,  $\rho$  and  $K$  are wave frequency, fluid density, and bulk modulus, respectively. The nodal region is of lowest pressure, thus, we apply  $\partial P/\partial x = 0$ , which yields to

$$-2kp_0 \exp(ikL/2) \sin(kx) = 0. \quad (2)$$

Apparently, at the center position of the microchannel ( $x = 0$ ), the pressure becomes minimum, which is  $p_{x=0} = 2p_0 \exp(-\omega\sqrt{|\rho/K|}L/2)$ .

The calculated field distribution of the evanescent wave is shown in Fig. 3, in which nodal position and gradient field are also revealed. Consider that the top and down boundaries are acoustic hard walls, and  $\omega = 38.2$  kHz,  $L = 55$  mm,  $H = 7$  mm,  $\rho = -1000$  kg/m<sup>3</sup>,  $K = 2.2 \times 10^9$  Pa, as illustrated in Fig. 3(a), starts from the boundaries, wave amplitude decreases exponentially from  $8.9 \times 10^3$  Pa to a lowest level of

$1.6 \times 10^3$  Pa in the center. Figure 3(b) reveals the field gradients of the evanescent field (red line) and standing wave field (blue line) generated by the same excitation. One could easily find that the evanescent field gradient has maximum amplitude two times larger than standing wave field. As indicated by the blue dots and arrows, particles would experience changeable force during moving process in standing wave background, because the channel is too wide as compared to the standing wavelength. Instead, when driven by evanescent field, particles from either side of the channel will move constantly towards the center position.

Another distinct advantage pertains to the proposed metafluid channel is that only one nodal position exists, no matter what type of incidences from the two boundaries are excited. As can be found from Eq. (2),  $x = 0$  is the unique root, which signifies only one region exists in the channel, i.e., the center of the channel, where the acoustic field reaches minimum. Thus, the field gradient always points to the outward directions. Additionally, noting the wave vector is a pure imaginary number, there is no phase delay during the propagation of the evanescent wave, accordingly no phase synchrony requirement on the two actuators to ensure the nodal position locates in the center of the channel, which is another necessary step in usual acoustic particle focusing method based on standing waves.

Radiation force acting on particles in the channel can be estimated by classic theories. Since particles usually vibrately driven by the acoustic wave, time-averaged radiation force plays more important role on particle trajectories. The radiation force of a particle was well defined in documents,<sup>26,31</sup> which can be written as

$$F = \frac{2v\delta(1-\beta)}{1+\beta} \frac{\partial T}{\partial x} - v \frac{\partial V}{\partial x}, \quad (3)$$

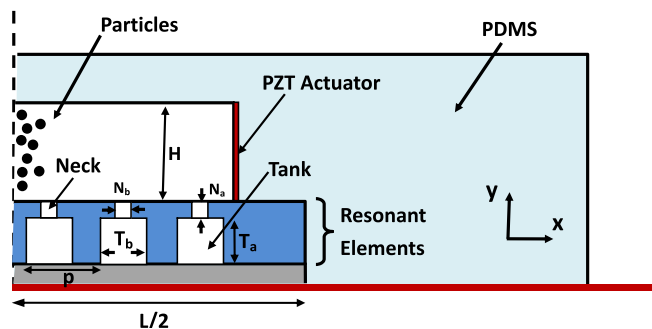


FIG. 2. The section plane of the microfluidic channel with acoustic resonant elements.

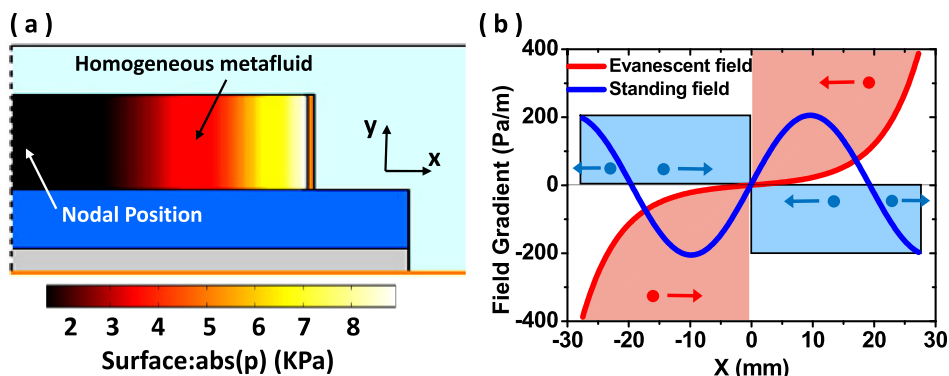


FIG. 3. (a) Pressure distribution of the acoustic wave in the microfluid with metamaterial fluid by a pair of the actuators from the channel sides, (b) gradients of evanescent field and standing wave under the same excitation and their resultant force directions.

where  $v = \pi r^2$  with  $r$  the radius of the particle, and  $\delta = \pi(a/2)^2(\beta - 1)/(\beta + 1)$ ,  $\beta = \rho_0/\rho_1$  with  $\rho_1$  the density of the particle,  $T$  and  $V$  are second-order approximations to the time-averaged densities of kinetic and potential energy of the incident field, respectively

$$T = (\rho_0/4)|\nabla P|^2 \text{ and } V = (\rho_0 k^2/4)|P|^2.$$

Massive particle movement driven by time-averaged radiation force in the acoustic metafield is simulated and displayed in Fig. 4. In the beginning, particles are released at the nodes of the numerical meshes among the metafluid. Radius of the particles are assumed to be  $\lambda/20$ , with density of  $1050 \text{ kg/m}^3$ . Viscosity of fluid is assumed to be  $0.001002 \text{ Pa}\cdot\text{s}$ , both the acoustophoretic force (radiation force) and drag force are taken into account for the particle movement, while the gravity is ignored. In Fig. 4(a), one can find that, at the start moment, the particles sit furthest from the center are exerted with the largest radiation force, about  $\pm 77 \text{ nN}$ . These forces

propel the particles to move with large acceleration, however, the speed of the particles is still small, as the fluid drag force will significantly consume the kinetic energy of the particles. After 20 s, the particles finally gather at the center of the channel within one tenth of the wavelength. The final forces acting on the particles then reduce to  $0.09 \text{ nN}$ , which are remarkably lower than that at the beginning, and thus, particles are stabilized in the center region.

The results derived from fluid with negative density can be well extended to the case of negative bulk modulus, according to duality of these two parameters in acoustic wave equations. Figure 4(b) shows similar particle focusing in a homogeneous negative bulk modulus fluid. Small difference of particle acoustophoresis forces between Figs. 4(a) and 4(b) can be observed, which is determined by the relation of density or bulk modulus between the particles and background fluid. Based on the theoretical analysis, we designed a structured channel that enables the fluid therein to have a similar response to acoustic incidence. We employed Helmholtz resonators to tune the behaviour of the fluid in the channel, making the fluid response as an effective fluid with negative bulk modulus.<sup>21</sup> A sectional view of the Helmholtz resonator is shown in Fig. 2, with tanks connected to the channel via small necks. This type of fluidic channel has been profoundly

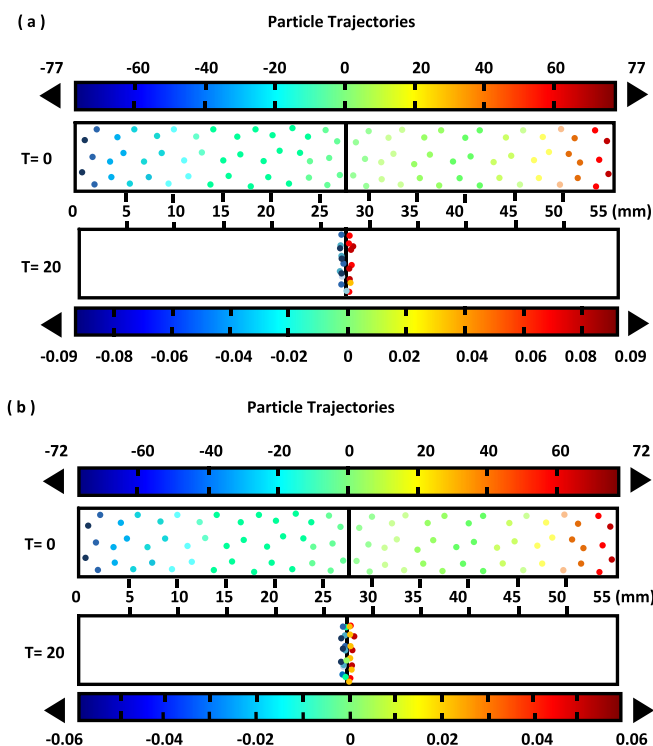


FIG. 4. Particles focusing in the center of the microchannel with metamaterial fluid after 20 s of the acoustic wave incidence, (a) fluid with negative density, (b) fluid with negative bulk modulus.

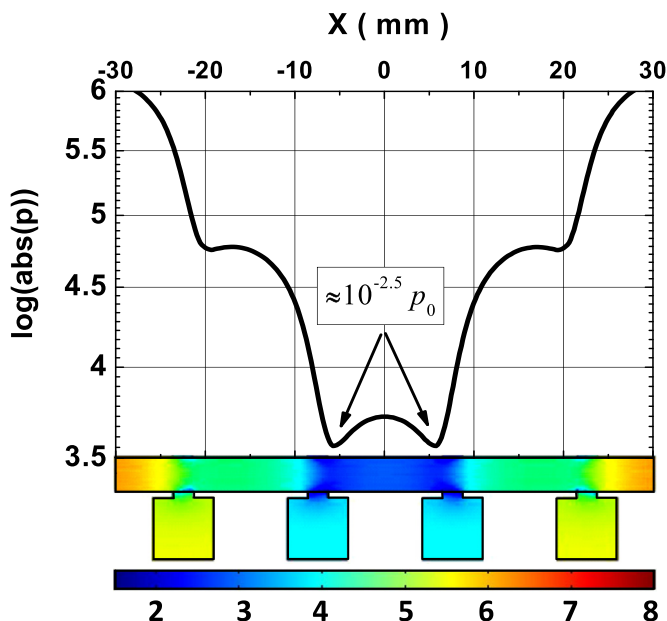


FIG. 5. Pressure amplitude distribution of the acoustic wave in the microfluid with resonant elements by a pair of the actuators from the channel sides.

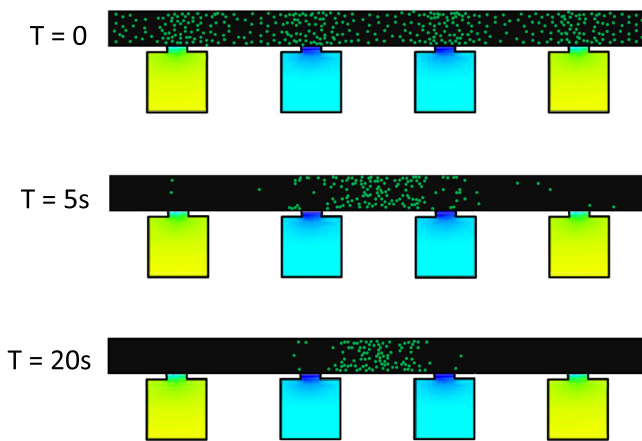


FIG. 6. Particles focusing process in the microfluidic channel with resonant elements. After 5 s of the acoustic wave incidence, obvious particle aggregation can be observed.

investigated and proved to have effectively negative bulk modulus,<sup>21</sup> while in some cases may also reveal negative density.<sup>32</sup> Since either negative bulk modulus or negative density can be equally harnessed for generating evanescent field and thus leading to particle focusing, here we concentrate on adapting the parameters of Helmholtz resonators to obtain the required acoustic field distribution.

Figure 5 shows the pressure distribution in the microchannel under illuminations of a pair of actuators at the lateral boundaries. Structural parameters for the channel and resonators are:  $L = 60$  mm,  $H = 4$  mm,  $N_a = 0.7$  mm,  $N_b = 2.2$  mm,  $T_a = 6.6$  mm,  $T_b = 6.6$  mm,  $p = 15$  mm,  $\omega = 38.2$  kHz. One could readily find that the field also decays exponentially toward the center of the channel and reduces to a level of  $10^{-2.5}p_0$ , although the gradient is not decreasing smoothly due to the sharp pressure variation at the necks of the resonators.

Based on the field distribution in the resonant channel, particle movement driven by the radiation force is simulated and illustrated in Fig. 6. Again large initial radiation forces were observed to act on the particles near the boundaries, about  $167 \mu\text{N}$ . Particles located close to the neck of the resonator have relative small force. After 5 s, the majority of the particles already move to the center region, only a small part of them are still trapped in the vicinities of the necks. After 20 s, most particles finally aggregate in the center region of the channel within  $\lambda/5$ .

According to Fig. 5, each Helmholtz resonator functions locally and independently to decay the acoustic field as the wave travels by. Therefore, a two dimensional array of Helmholtz resonators in Fig. 1 actually can be well exploited to generate a nodal point in the middle of the plane above these resonators, if another two actuators excite waves from Z direction (noting that currently the waves are excited from X direction). Accordingly, two-dimensional particle focusing can be readily achieved. Other metamaterial<sup>33,34</sup> may also be served to realize a 2D particle focusing by carefully arranging them into suitable positions.

A particle focusing microchannel model was designed employing the acoustic radiation force of particles experienced

in evanescent field. Field distribution of evanescent wave in acoustic homogeneous metafluid was studied, and radiation force acting on particles were also investigated. Then particle movements in the metafluid were simulated, in which particles were confined in a region of less than one tenth of wavelength. By replacing the homogeneous metafluid with Helmholtz resonators, evanescent acoustic field was also found in the structural channel, particle focusing phenomenon was also observed, with a confining region of one fifth of the wavelength.

This work was supported by Natural Science and Engineering Research Council of Canada (NSERC), and in part by the National Natural Science Foundation of China under Grant No. 11002023, and BIT Science Foundation under Grant No. 20090142011.

- <sup>1</sup>N. Sundararajan, M. S. Pio, L. P. Lee, and A. A. Berlin, *J. Microelectromech. Syst.* **13**(4), 559–567 (2004).
- <sup>2</sup>C. Simonnet and A. Groisman, *Appl. Phys. Lett.* **87**(11), 114104 (2005).
- <sup>3</sup>R. Yang, D. L. Feedback, and W. Wang, *Sens. Actuators, A* **118**(2), 259–267 (2005).
- <sup>4</sup>S. C. Jacobson and J. M. Ramsey, *Anal. Chem.* **69**(16), 3212–3217 (1997).
- <sup>5</sup>A. Y. Fu, C. Spence, A. Scherer, and F. H. Arnold, *Nat. Biotechnol.* **17**(11), 1109–1111 (1999).
- <sup>6</sup>D. Erickson, X. Liu, R. Venditti, D. Li, and U. J. Krull, *Anal. Chem.* **77**(13), 4000–4007 (2005).
- <sup>7</sup>A. J. Chung, D. Kim, and D. Erickson, *Lab Chip* **8**(2), 330–338 (2008).
- <sup>8</sup>C. Yu, J. Vykoukal, D. Vykoukal, J. Schwartz, L. Shi, and P. Gascoyne, *J. Microelectromech. Syst.* **14**(3), 480–487 (2005).
- <sup>9</sup>D. Holmes, H. Morgan, and N. Green, *Biosens. Bioelectron.* **21**(8), 1621–1630 (2006).
- <sup>10</sup>H. Chu, I. Doh, and Y. Cho, *Lab Chip* **9**(5), 686–691 (2009).
- <sup>11</sup>C. Liu, L. Lagae, and G. Borghs, *Appl. Phys. Lett.* **90**(18), 184109 (2007).
- <sup>12</sup>A. Nilsson, F. Petersson, H. Jönsson, and T. Laurell, *Lab Chip* **4**(2), 131–135 (2004).
- <sup>13</sup>G. R. Goddard, C. K. Sanders, J. C. Martin, G. Kaduchak, and S. W. Graves, *Anal. Chem.* **79**(22), 8740–8746 (2007).
- <sup>14</sup>F. Petersson, A. Nilsson, C. Holm, H. Jönsson, and T. Laurell, *Lab Chip* **5**(1), 20–22 (2005).
- <sup>15</sup>P. G. Erlandsson and N. D. Robinson, *Electrophoresis* **32**(5), 784–790 (2011).
- <sup>16</sup>S. Rodamporn, N. R. Harris, S. P. Beeby, R. J. Boltryk and T. Sanchez-Elsner, *IEEE Trans. Biomed. Eng.* **58**(4), 927–934 (2011).
- <sup>17</sup>V. G. Veselago, *Sov. Phys. Usp.* **10**(4), 509 (1968).
- <sup>18</sup>R. A. Shelby, D. R. Smith, and S. Schultz, *Science* **292**(5514), 77 (2001).
- <sup>19</sup>J. B. Pendry, *Phys. Rev. Lett.* **85**(18), 3966 (2000).
- <sup>20</sup>Z. Y. Liu, X. X. Zhang, Y. W. Mao, Y. Y. Zhu, Z. Y. Yang, C. T. Chan, and P. Sheng, *Science* **289**(5485), 1734–1736 (2000).
- <sup>21</sup>N. Fang, D. Xi, J. Xu, M. Ambati, C. Sun, and X. Zhang, *Nature Mater.* **5**(6), 452–456 (2006).
- <sup>22</sup>J. Li and C. T. Chan, *Phys. Rev. E* **70**(5), 055602 (2004).
- <sup>23</sup>Z. Yang, J. Mei, M. Yang, N. H. Chan, and P. Sheng, *Phys. Rev. Lett.* **101**(20), 204301 (2008).
- <sup>24</sup>J. Zhu, J. Christensen, J. Jung, L. Martín-Moreno, X. Yin, L. Fok, X. Zhang, and F. J. García-Vidal, *Nat. Phys.* **7**(1), 52–55 (2011).
- <sup>25</sup>X. N. Liu, G. K. Hu, G. L. Huang, and C. T. Sun, *Appl. Phys. Lett.* **98**(25), 251907 (2011).
- <sup>26</sup>L. V. King, *Proc. R. Soc. London, Ser. A* **147**(861), 212–240 (1934).
- <sup>27</sup>T. F. W. Embleton, *J. Acoust. Soc. Am.* **26**(1), 40–45 (1954).
- <sup>28</sup>L. P. Gor'kov, *Sov. Phys. Dokl.* **6**(9), 773–775 (1962).
- <sup>29</sup>E. Leung, N. Jacobi, and T. Wang, *J. Acoust. Soc. Am.* **70**(6), 1762–1767 (1981).
- <sup>30</sup>M. Bruneau, *Fundamentals of Acoustics* (ISTE Ltd, London, 2006).
- <sup>31</sup>J. Wu, G. H. Du, S. S. Work, and D. M. Warshaw, *J. Acoust. Soc. Am.* **87**(2), 581–586 (1990).
- <sup>32</sup>Y. Cheng, J. Y. Xu, and X. J. Liu, *Phys. Rev. B* **77**(4), 045134 (2008).
- <sup>33</sup>J. Christensen, L. Martín-Moreno, and F. J. García-Vidal, *Appl. Phys. Lett.* **97**(13), 134106 (2010).
- <sup>34</sup>J. S. Bell, I. R. Summers, A. R. J. Murray, E. Hendry, J. R. Sambles, and A. P. Hibbins, *Phys. Rev. B* **85**(21), 214305 (2012).